

ORIGINAL ARTICLE

Expanding the genetic landscape of oral-facial-digital syndrome with two novel genes

Alanna Strong^{1,2}  | Laurie Simone³ | Anthony Krentz⁴ | Courtney Vaccaro² |
Deborah Watson² | Hayley Ron¹ | Jennifer M. Kalish^{1,5}  | Helio F. Pedro³ |
Elaine H. Zackai^{1,5} | Hakon Hakonarson^{1,2,5,6} 

¹Division of Human Genetics, Children's Hospital of Philadelphia, Philadelphia, Pennsylvania

²The Center for Applied Genomics, Children's Hospital of Philadelphia, Philadelphia, Pennsylvania

³Center for Genetic and Genomic Medicine, Hackensack University Medical Center, Hackensack, New Jersey

⁴PreventionGenetics, Marshfield, Wisconsin

⁵Department of Pediatrics, Perelman School of Medicine, University of Pennsylvania, Philadelphia, Pennsylvania

⁶Division of Pulmonary Medicine, Children's Hospital of Philadelphia, Philadelphia, Pennsylvania

Correspondence

Hakon Hakonarson, Director, Center for Applied Genomics, Investigator, The Joseph Stokes, Jr. Research Institute, Children's Hospital of Philadelphia Endowed Chair in Genomic Research, Professor of Pediatrics, Perelman School of Medicine at the University of Pennsylvania, 3615 Civic Center Boulevard, Philadelphia, PA 19104, USA.
Email: hakonarson@email.chop.edu

Funding information

Medical Genetics Research Training Grant, Grant/Award Number: 5T32GM008638-22; Institutional Development Fund

Abstract

Oral-facial-digital syndromes (OFDS) are a heterogeneous and rare group of Mendelian disorders characterized by developmental abnormalities of the oral cavity, face, and digits caused by dysfunction of the primary cilium, a mechanosensory organelle that exists atop most cell types that facilitates organ patterning and growth. OFDS is inherited both in an X-linked dominant, X-linked recessive, and autosomal recessive manner. Importantly, though many of the causal genes for OFDS have been identified, up to 40% of OFD syndromes are of unknown genetic basis. Here we describe three children with classical presentations of OFDS including lingual hamartomas, polydactyly, and characteristic facial features found by exome sequencing to harbor variants in causal genes not previously associated with OFDS. We describe a female with hypothalamic hamartoma, urogenital sinus, polysyndactyly, and multiple lingual hamartomas consistent with OFDVI with biallelic pathogenic variants in *CEP164*, a gene associated with ciliopathy-spectrum disease, but never before with OFDS. We additionally describe two unrelated probands with postaxial polydactyly, multiple lingual hamartomas, and dysmorphic features both found to be homozygous for an identical *TOPORS* missense variant, c.29 C>A; (p.Pro10Gln). Heterozygous *TOPORS* pathogenic gene variants are associated with autosomal dominant retinitis pigmentosa, but never before with syndromic ciliopathy. Of note, both probands are of Dominican ancestry, suggesting a possible founder allele.

KEYWORDS

CEP164, ciliopathy, oral-facial-digital syndrome, *TOPORS*

1 | INTRODUCTION

Ciliopathy syndromes are rare Mendelian disorders caused by dysfunction of the primary cilium, a mechanosensory organelle that exists atop most cell types that facilitates proper organ patterning and

growth (Berbari et al., 2009; Fry et al., 2014). Oral-facial-digital syndromes (OFDS) represent a heterogeneous group of ciliopathies, characterized by the core features of oral cavity malformations, such as tongue hamartomas, cleft palate, lobulated tongue, and hyperplastic frenula, craniofacial dysmorphisms such as down-slanted palpebral

This is an open access article under the terms of the Creative Commons Attribution License, which permits use, distribution and reproduction in any medium, provided the original work is properly cited.

© 2021 The Authors. *American Journal of Medical Genetics Part A* published by Wiley Periodicals LLC.

fissures, hypertelorism, and broad and flat nasal bridge, and digit malformations such as brachydactyly, polydactyly, and syndactyly (Gurrieri et al., 2007). Affected individuals can also have mild to severe intellectual impairment, structural brain differences, hypothalamic hamartoma, facial milia, coloboma, retinopathy, missing, extra or defective teeth, clinodactyly, structural heart differences, and polycystic kidneys (Bruel et al., 2017; Franco & Thauvin-Robinet, 2016). Importantly, features of OFDS can be seen in other ciliopathy syndromes, most commonly Joubert syndrome (JS), which is defined by the clinical triad of hypotonia, developmental delays, and a pathognomonic cerebellar and brain stem malformation referred to as a “molar tooth sign” (MTS) (Parisi & Glass, 2003).

Since its initial description in 1941 (Mohr, 1941), multiple OFDS types have been described with significant phenotypic overlap but with distinct patterns of organ system involvement and malformations (Bruel et al., 2017; Franco & Thauvin-Robinet, 2016). OFD is inherited in an X-linked dominant, X-linked recessive, and autosomal recessive manner. Causal genes have not been identified for approximately 40% of OFD types (Bruel et al., 2017; Franco & Thauvin-Robinet, 2016).

Here we describe three probands with a clinical diagnosis of OFDS VI. One patient was compound heterozygous for nonsense and frameshift *CEP164* variants, and two unrelated probands of Dominican Republic descent were homozygous for a c.29 C>A; p.(Pro10Gln) missense variant in *TOPORS*. We propose that *CEP164* and *TOPORS* are novel causal genes for OFD VI, and suggest that the c.29 C>A allele is may represent a founder allele in the Dominican Republic population.

2 | METHODS

2.1 | Editorial policies and ethical considerations

All individuals and families agreed to participate in this study and signed appropriate consent forms. Permission for clinical photographs was given separately. This study was approved by the institutional IRB (Protocol # 16–013278).

2.2 | Genetic testing methodology

Chromosomal microarray for Patient 1 was performed at SUNY Upstate Medical University. Trio exome sequencing was performed on DNA from Patient 1 at GeneDx. Prenatal chromosomal microarray and Joubert Syndrome panel testing was performed on Patient 2 at GeneDx. Trio exome sequencing was performed for Patient 2 at PreventionGenetics. Prenatal chromosomal microarray and trio exome sequencing was performed for Patient 3 at GeneDx and for his affected sibling at Integrated Genetics. Patient 3 was recruited into the Center for Applied Genomics (CAG) at CHOP for exome reanalysis. Patients 2 and 3 were matched through GeneMatcher (Sobreira et al., 2015).

2.3 | Exome sequencing reanalysis

Under an Institutional Review Board approved protocol (Protocol # 16-013278), informed consent was obtained from the family of Patient 3 for enrollment in CAG. Variant annotation, filtration and prioritization was performed with GDCross, a variant annotation and prioritization platform developed within CAG. Variants with $\geq 5\times$ coverage were initially filtered at 0.5% gnomAD MAF and annotated with a combination of multiple tools and databases, including Variant Effect Predictor, HGMD, ClinVar, dbSNP, OMIM, HPO, PolyPhen-2 and SIFT, and a custom-built splice-site annotator. The list of patient variants is filtered against the pedigree and HPO terms describing the patient's phenotype, and GDCross assigns each variant a priority score of likelihood as the causal variant for the patient's disease. Variants are ranked using a weighted combination of multiple factors, including (a) overlap with HPO terms, (b) patient and family genotypes, (c) predicted functional impact, (d) inheritance modeling, and (e) presence in mutation databases such as HGMD and ClinVar.

3 | RESULTS

3.1 | Patient cohort

3.1.1 | Patient 1

Patient 1 was the product of a naturally-conceived pregnancy to a then 40-year-old G5P3→4 mother. Family history was notable for a 12-year-old brother with Trisomy 21 (conceived at 27 years of age) and a 14-year-old sister with suspected autoimmune aplastic anemia status post bone marrow transplant. There were no medications or exposures during the pregnancy. Noninvasive prenatal testing was done due to maternal age and was normal. Twenty-week ultrasound was also normal. An additional ultrasound was done at 29 weeks due to loss of the cervical mucus plug, and was notable for multiple congenital anomalies, prompting fetal MRI and echocardiogram, which were notable for polydactyly, brain cyst, absent vagina, and hydronephrosis. Patient was ultimately born via caesarian section at 33 weeks gestational age due to fetal tachycardia and worsening hydronephrosis. Birth weight was 3.115 kg (>97%; 50% for 36 weeks gestational age) and birth length was 43 cm (25–50%). She was admitted to the NICU for management. She was noted to have hypotonia, four-extremity polydactyly, syndactyly of multiple digits, multiple tongue hamartomas, and urogenital sinus. A suprapubic catheter was placed with improvement in her hydronephrosis and hydrometrocolpos. Echocardiogram and ophthalmology examination were normal. Head ultrasound showed a prominent temporal horn of the left lateral ventricle. Brain MRI showed hypothalamic hamartoma and asymmetric ventriculomegaly.

She was evaluated by Genetics at 3 months of age. Growth parameters were notable for a weight of 3.65 kg (10–25% corrected), height of

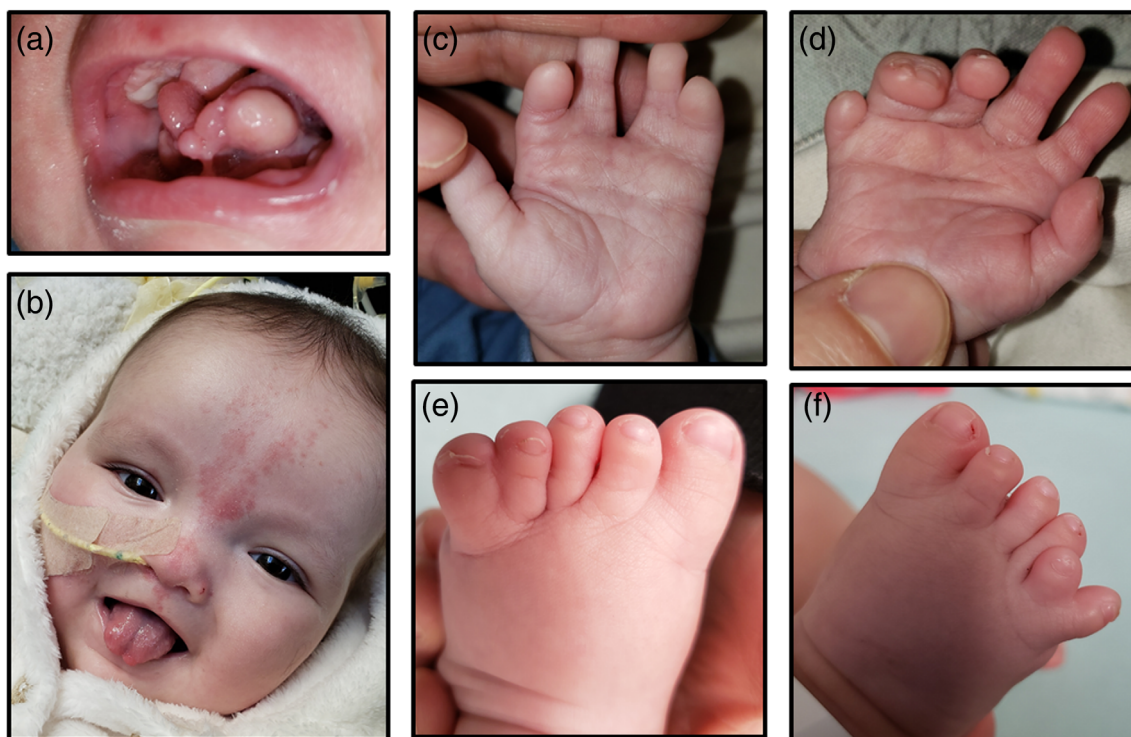


FIGURE 1 (a) Patient 1 oral cavity at 3 months of age demonstrating multiple lingual hamartomas and accessory frenula. (b) Patient 1 oral cavity at 6 months of age after hamartoma resection showing bifid tongue. Facial features notable for hypertelorism, broad nasal bridge and nevus simplex. (c) Patient 1 left hand showing 2,3 and 4,5 syndactyly. (d) Patient 1 right hand showing postaxial polydactyly and 5,6 syndactyly. (e) Left foot showing post axial polydactyly with complete 5,6 syndactyly. (f) Patient 1 right foot notable for postaxial polydactyly [Color figure can be viewed at wileyonlinelibrary.com]

48.3 cm (<3%; 50% for newborn), and head circumference of 36.5 cm (75% corrected). Physical examination was notable for hypotonia, relative macrocephaly, down-slanting palpebral fissures, hypertelorism, broad and flat nasal bridge, upper alveolar ridge notch, multiple lingual hamartomas, accessory frenula, high palate, mild micrognathia, and linear nevus simplex extending from the forehead to the upper lip (Figure 1a,b). Extremity examination was notable for a left hand with 2,3 and 4,5 syndactyly (Figure 1c), postaxial polydactyly of the right hand with 7 digits total and complete syndactyly of digits 5,6 (Figure 1d), postaxial polydactyly with complete 5,6 syndactyly of the left foot (Figure 1e), and postaxial polydactyly of the right foot (Figure 1f).

Presence of hypothalamic hamartoma, lingual hamartomas, polydactyly, and syndactyly was concerning for OFD VI (Poretta et al., 2012). Kidney ultrasound was performed, which showed moderate, symmetric hydronephrosis with no kidney cysts. An EEG was performed, which showed intermittent focal slowing in the bifrontal region and rare epileptiform discharges in the left temporal and right occipital regions. She underwent surgical removal of her lingual hamartomas and accessory frenula, and was admitted postoperatively due to concern for silent aspiration, later confirmed on video swallow study. She is currently NPO. Patient is now 6 months of age, gestationally corrected to 4 months of age. Motor milestones are delayed with minimal head control. Social skills are normal; patient fixes and follows, smiles, and is extremely interactive.

3.1.2 | Patient 2

Patient 2 was born to a 31-year-old G4P3→4 mother. Family history was noncontributory. Both parents were from the Dominican Republic. Pregnancy was complicated by gestational diabetes treated with metformin. Prenatal ultrasounds and follow up fetal MRI were notable for four extremity polydactyly, severely hypoplastic/absent cerebellar vermis, mildly enlarged posterior fossa, and micropenis. Patient was born via repeat caesarian section at 38 weeks gestational age. APGARS were 9 and 9 at 1 and 5 min of life, respectively. Birth weight was 3.73 kg (90%), birth length was 50.5 cm (75–90%), and head circumference was 37 cm (>97%). Patient was diagnosed postnatally with hypotonia, multiple lingual hamartomas, four-extremity postaxial polydactyly, and micropenis. Echocardiogram demonstrated pulmonic valve stenosis, tricuspid valve regurgitation, and patent foramen ovale. MRI demonstrated arachnoid cyst and MTS.

Genetics evaluated the baby at 1 day of life and again at 4 months of life. At 4 months of life, weight was 8.9 kg (>97%; 50% for 9 months), length was 60.5 cm (25%), and head circumference was 44 cm (98%). Physical examination was notable for bilateral ptosis worse on the left, down-slanting palpebral fissures, broad nasal bridge, slightly low and posteriorly-rotated ears, multiple lingual hamartomas, 2/6 murmur, and hypotonia with significant head lag. Patient did not

fix or follow. Kidney ultrasound was normal, and ophthalmology examination was performed, but the results are unknown. Patient is currently 10 months of age. Clinical course is complicated by severe developmental delay.

3.1.3 | Patient 3

Patient 3 was the product of a naturally-conceived pregnancy to a then 21-year-old G2P0→1 mother. Both parents were from the Dominican Republic. Family history was notable for consanguinity with the mother's maternal grandfather and the father's paternal grandmother being siblings (second-cousin union) and for a prior pregnancy terminated for multiple congenital anomalies, including lemon-shaped head with frontal bossing, posterior fossa cyst, encephalocele, and arthrogryposis with bilateral talipes equinovarus. Microarray and exome sequencing were nondiagnostic.

Pregnancy was complicated by prenatal ultrasound concerning for multiple congenital anomalies, prompting fetal MRI, which demonstrated bilateral ventriculomegaly, dandy-walker malformation, occipital meningocele, ambiguous genitalia, bilateral talipes equinovarus, and shortened long bones. Patient was born at 36 weeks gestational age via caesarian section for fetal macrocephaly. APGARs were 2 and 8 and 1 and 5-min of life, respectively. Birth weight was 3.17 kg (75%), birth length was 45 cm (20%), and head circumference was 42 cm (>97%). He was diagnosed postnatally with cleft palate and four-extremity polydactyly. He developed respiratory distress in the delivery room requiring positive pressure ventilation, and was intubated shortly thereafter for persistent apneas and desaturations.

He was evaluated by Genetics on day of life 3. Physical examination was notable for macrocephaly with prominent forehead and occiput, down-slanting palpebral fissures, hypertelorism, nasal milia, bifid tongue, lingual hamartomas, micrognathia, four-extremity postaxial polydactyly, micropenis and hypotonia. Due to concern for OFDS, an abdominal ultrasound, echocardiogram, brain MRI and ophthalmology examination were requested. Abdominal ultrasound showed structurally normal liver and kidneys, echocardiogram showed a structurally normal heart, ophthalmology examination showed bilateral optic nerve colobomas, and brain MRI showed dandy-walker malformation, left parasagittal occipital encephalocele, possible ectopic posterior pituitary gland, possible left frontal lobe cleft, and small optic nerves.

Patient is currently 8-months of age. Growth parameters are notable for a weight of 10.5 kg (95%), a height of 61 cm (<3%; 50% for 2.5 months of age), and a head circumference of 46 cm (>97%). Physical examination is largely unchanged. Patient's clinical course has been complicated by hydrocephalus status post shunt placement complicated by multiple shunt infections, respiratory failure status post tracheostomy placement, G-tube dependence, cortical visual impairment, neuro-irritability, spasticity, central adrenal insufficiency, and profound developmental delay.

3.2 | Genetics testing

3.2.1 | Patient 1

Patient 1 had a chromosomal microarray performed, which showed a 470 base pair duplication of unclear clinical significance at 5q35.2 (hg19: 175,668,563–176,138,247) including the *NOP16*, *FAF2*, *SIMC1*, *CLTB*, and *SNCB* genes. Parental testing was declined. Trio exome sequencing was performed at GeneDx, and was notable for a paternally-inherited pathogenic *CEP164* frameshift variant (c.2535_2536dupGG; p.Glu846Glyfs*10) and a maternally-inherited pathogenic *CEP164* non-sense variant (c.3055 C>T; p.Gln1019*).

3.2.2 | Patient 2

Patient 2 had a prenatal microarray and JS gene panel performed at GeneDx, which were nondiagnostic. Trio exome sequencing was performed postnatally at PreventionGenetics, and was notable for biallelic missense variants of uncertain significance in the candidate gene *TOPORS* (c.29 C>A; p.Pro10Gln) and a 6 Mb region of homozygosity on chromosome 9 (hg19: 32,425,909–38,423,826) including the *TOPORS* gene.

3.2.3 | Patient 3

Patient 3 had a prenatal microarray and trio exome sequencing performed at GeneDx. Microarray was notable for two regions of homozygosity on chromosomes 8 (hg19: 128,664,940–140,805,582) and 9 (hg19: 22,920,663–40,087,758) but no copy number variations. Exome sequencing was notable for a paternally-inherited pathogenic variant in *PMM2* (c.713G>A; p.(Arg238His)), associated with the autosomal recessive congenital disorder of glycosylation *PMM2*-CDG. Microarray and trio exome sequencing were also performed on the previously affected fetus. Microarray was notable for two regions of homozygosity on chromosomes 7 (hg19: 44,098,864–58,019,983) and 9 (hg19: 25,000,261–40,087,758). Patient and family were enrolled in CAG for research exome reanalysis given negative clinical testing. Reanalysis revealed biallelic variants of uncertain significance in *TOPORS* (c.29 C>A; p.Pro10Gln) in the affected proband. These variants were clinically confirmed via gene sequencing at PreventionGenetics. Integrated Genetics subsequently confirmed that the affected fetus also harbored the *TOPORS* variants. The Pro10Gln variant was subsequently upgraded to likely pathogenic for both patients by PreventionGenetics given the similar clinical presentations and identical variants. Of note, *TOPORS* maps to the region of homozygosity shared by both children.

4 | DISCUSSION

Oral facial digital syndromes (OFDS) are a group of rare ciliopathy syndromes characterized by the core features of oral cavity

TABLE 1 Tabulated view of phenotypes associated with 14 different OFD syndromes as compared to the phenotypes of our described patients [Color table can be viewed at wileyonlinelibrary.com]

	I	II	III	IV	V	VI	VII	VIII	IX	X	XI	XII	XIII	XIV	Pt 1	Pt 2	Pt 3
Genetics																	
Gene	OFD1	NEK1	TMEM231	TCTN3	DDX59	C5OR F42 CPLANE1 OFD1 TMEM107 TMEM216	Unk	Unk	SCLT1 TBC 1D32	Unk	Unk	Unk	Unk	C2CD3	CEP164	TOPORS	TOPORS
Inheritance	XLD	AR	AR	AR	AR	AR	XLD	XLR	XLR	AD	Unk	Unk	Unk	AR	AR	AR	AR
Craniofacial features																	
Hypertelorism	+	+	+	+	+	+	+	+			+	+	+		+		+
Telecanthus										+				+			
Cleft lip	+	+			+	+	+	+	+				+				
Cleft palate	+	+		+		+	+	+	+	+	+	+	+	+	+	+	+
Accessory frenulae	+	+	+	+		+	+	+	+	+	+	+	+	+	+	+	+
Lobulated tongue	+	+	+	+		+	+	+	+	+	+	+	+	+	+	+	+
Cleft tongue	+	+										+		+	+	+	+
Lingual hamartomas	+	+		+			+	+	+				+	+	+	+	+
Tooth defects	+		+									+		+	+	+	+
Bi-rod uvula			+														
Micrognathia				+		+											+
Musculoskeletal features																	
Polydactyly	+		+	+	+	+	+	+	+	+	+	+	+	+	+	+	+
Clinodactyly	+	+				+	+	+	+				+				
Brachydactyly	+	+		+					+				+				
Syndactyly	+			+		+							+		+		
Oligodactyly										+							
Fibular aplasia										+							
Short stature	+	+		+		+		+	+						+	+	+
Neurological involvement																	
Corpus callosum agenesis	+			+									+		+		
Ventriculomegaly	+	+										+	+		+		+
Molar tooth sign				+		+							+		+		+
Cerebellar vermis hypoplasia	+		+	+									+		+	+	+
Hypothalamic Hamartoma	+					+								+			
Heterotopia																	
Neural tube defect				+		+							+				+
Intellectual disability	+		+	+	+	+	+	+	+		+	+		+	+	+	+
Other Organ involvement																	
Congenital heart disease												+	+				+
Kidney disease	+		+	+		+	+								+		
Liver disease	+																
Hearing loss												+					
Structural eye differences									+								+

Notes: Overlapping features are highlighted in red. Given the hypertelorism, lingual hamartomas, tongue lobulations, polysyndactyly, hypothalamic hamartoma, neural tube defects, molar tooth sign and intellectual disability seen in our patients, we propose that our patients' phenotypes are most consistent with OFD VI.

malformations, facial dysmorphisms, and digit anomalies (Bruel et al., 2017; Franco & Thauvin-Robinet, 2016). OFDS subtypes are classified based on pattern of associated features such as structural brain differences, intellectual disability, skeletal differences, congenital heart disease and kidney disease, with over 18 subtypes described to date (Table 1).

Over 16 genes have now been identified as causal for OFDS (Bruel et al., 2017). These genes encode components of the primary cilium, a mechanosensory organelle that facilitates organ growth and patterning (Berbari et al., 2009; Fry et al., 2014). OFDS genes localize to virtually every ciliary subsegment, including the basal body, centriole, transition zone, and axoneme (Figure 2). The exact mechanism by which ciliary dysfunction causes the clinical features of OFDS is unknown.

Though initially described 80 years ago, up to 40% of the described OFDS subtypes do not have an associated gene and many patients with a clinical diagnosis of OFDS have negative molecular testing, highlighting our incomplete understanding of the genetic landscape of these conditions (Bruel et al., 2017; Franco & Thauvin-Robinet, 2016). Additionally, many genes associated with OFDS are also associated with other ciliopathy syndromes, most commonly JS; however, genotype-phenotype correlation remains elusive, and it is difficult to use mutation type to predict which ciliopathy phenotype a patient will ultimately have (Lambacher et al., 2016; Shaheen et al., 2013; Valente et al., 2010).

Here we describe two novel genes identified in patients with clinical features consistent with OFD VI: *CEP164*, previously identified as causal for the ciliopathies nephronophthisis, JS and Bardet Biedl syndrome, and *TOPORS*, a gene associated with the autosomal dominant ciliopathy RP, but never before with syndromic ciliopathy.

CEP164 maps to 11q23.3 and encodes centrosomal protein of 164 kDa, a component of the centriolar distal appendage. *CEP164* is required for vesicular docking at the centriole, thereby enabling ciliogenesis (Graser et al., 2007). *CEP164* has also been associated with coordination of the DNA damage response (Pan & Lee, 2009; Sivasubramaniam et al., 2008); however, this has recently been challenged (Daly et al., 2016). Morpholino-mediated *cep164* knockdown in zebrafish disrupts the DNA damage pathway and causes nephronophthisis-spectrum disease and hydrocephalus (Chaki et al., 2012). Total body *cep164* deficiency is embryonic lethal in mice, associated with holoprosencephaly, abnormal heart development, and gross patterning defects, and conditional *cep164* deficiency in multiciliated cells causes hydrocephalus, lung disease, and infertility, supporting a role for *CEP164* in ciliary function (Siller et al., 2017). Biallelic *CEP164* variants have been identified in multiple individuals affected by ciliopathy-spectrum disease, including Leber congenital amaurosis, Bardet-Biedl syndrome, and JS with associated features including obesity, bronchiectasis, liver fibrosis, and intellectual disability (Chaki et al., 2012; Shamseldin et al., 2020). Pathogenic *CEP164*

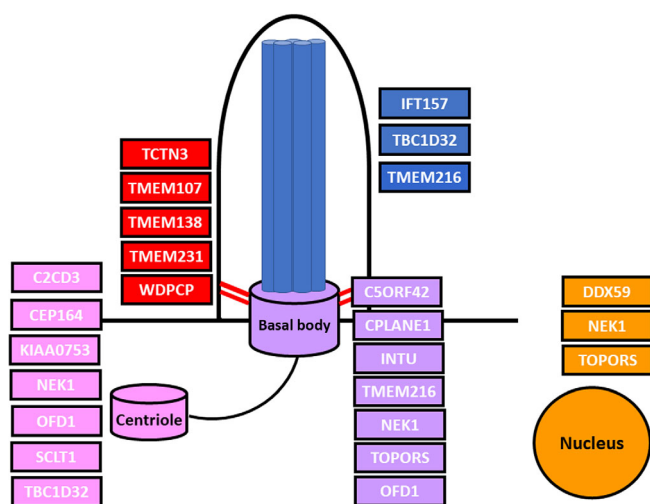


FIGURE 2 Genes associated with OFDS localize to multiple ciliary sub-compartments. The primary cilium is anchored to the cell by the basal body (purple), which is formed from the mother centriole and remains associated with its centriole pair (pink). The transition zone (red) serves as the gatekeeper for the cilium to control entry and exit. The axoneme (blue) is composed of microtubule doublets that provides structure to the cilium and also forms the framework for ciliary transport. The nucleus (orange) is an important target of ciliary signaling (EHZ) [Color figure can be viewed at [wileyonlinelibrary.com](#)]

variants are believed to cause ciliopathy-spectrum disease by disrupting ciliogenesis and possibly also through modulation of the DNA damage response and cell cycle control (Chaki et al., 2012; Graser et al., 2007; Pan & Lee, 2009; Sivasubramaniam et al., 2008). We hypothesize that Patient 1 presented with severe ciliopathy-spectrum disease because her nonsense and frameshift *CEP164* variants more significantly impair *CEP164* function. Indeed, patients with biallelic nonsense *CEP164* variants presented with Bardet-Biedl and JS phenotypes, as opposed to patients harboring missense variants, who presented with nephronophthisis and retinal disease (Chaki et al., 2012; Shamseldin et al., 2020).

TOPORS maps to 9p21.1 and encodes topoisomerase I-binding arginine/serine rich protein, a ubiquitously-expressed protein that localizes to the nucleus and basal body (Chakarova et al., 2011). *TOPORS* was originally identified in a screen for topoisomerase interacting proteins, and was later found to also interact with p53 (Haluska Jr et al., 1999; Zhou et al., 1999). *TOPORS* functions as an E3 ubiquitin ligase, and plays a role in protein ubiquitination and sumoylation (Pungaliya et al., 2007; Rajendra et al., 2004). Morpholino-mediated *topors* knockdown in zebrafish causes microphthalmia, kinked tail and body edema, all established ciliopathy phenotypes in fish (Chakarova et al., 2011). Heterozygous *TOPORS* variants are associated with the retinal ciliopathy retinitis pigmentosa (RP) (Bowne et al., 2008; Chakarova et al., 2007).

The mechanism by which heterozygous *TOPORS* variants cause disease is unknown. Biallelic *TOPORS* variants have not been previously reported. Given the localization of *TOPORS* at the ciliary base and in the nucleus, loss of *TOPORS* function could cause ciliopathy-spectrum disease by disrupting ciliary homeostasis directly or through

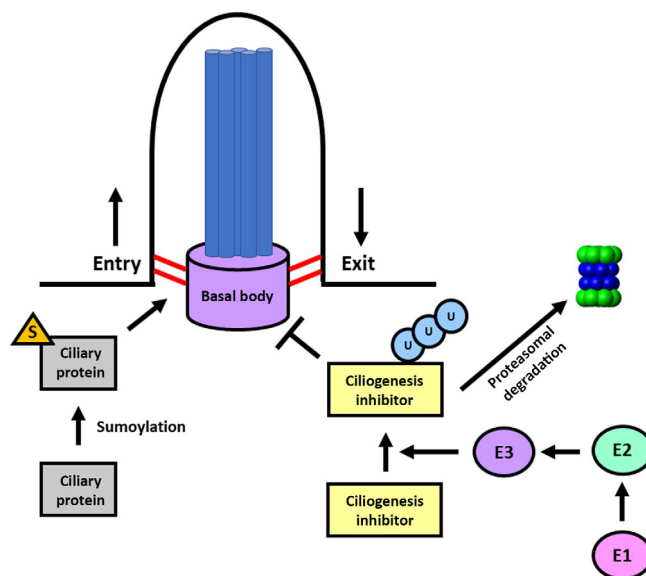


FIGURE 3 Proposed mechanism for *TOPORS*-spectrum disease. Center: The cilium is a hair-like appendage that exists atop most cell types. It consists of a basal body (purple), a modified centriole, which anchors the microtubules that make up the axoneme (blue) to the cell. The transition zone (red) at the ciliary base controls entry into the cilium. Right: E1 (pink), E2 (green), and E3 (purple) facilitate the transfer of ubiquitin to appropriate substrates to control ciliogenesis and ciliary function. Left: Many ciliary proteins undergo post-translational sumoylation to control their ciliary entry. *TOPORS* is an E3 ubiquitin ligase that also has sumoylation activity. We hypothesize that *TOPORS* deficiency disrupts ciliary function by interfering with ciliary protein ubiquitination and possibly sumoylation [Color figure can be viewed at [wileyonlinelibrary.com](#)]

dysregulated gene expression. We hypothesize that loss of *TOPORS* function disrupts ciliogenesis and ciliary function by interfering with the proper ubiquitination and turnover of ciliary proteins and morphogens (Figure 3). Disruption of the ciliary ubiquitin-proteasome system disrupts ciliogenesis, and biallelic variants in genes involved in regulation of the ubiquitin-proteasome system have been identified in ciliopathy patients (Gerhardt et al., 2015; Izawa et al., 2015; Kasahara et al., 2014).

All three *TOPORS* patients harbor identical biallelic missense variants (c.29 C>A; p.Pro10Gln) in *TOPORS*. *TOPORS* is intolerant to loss-of-function variants, with a pLI of 1. The Pro10Gln variant has been reported in gnomAD and ExAc at low allele frequency, and there are no homozygotes. In silico prediction tools such as polyphen and SIFT support pathogenicity. Given the overlapping patient phenotypes, the Pro10Gln variant was reclassified by PreventionGenetics as likely pathogenic. Interestingly, neither parent nor any relatives report vision difficulties or RP, suggesting that this variant is a hypomorph, insufficient to cause retinal disease in the heterozygous state, but severe enough to cause syndromic ciliopathy in the homozygous state.

Combined autosomal dominant and autosomal recessive inheritance has been reported for ciliopathies. Heterozygous *PKD1* variants are the most common cause of adult-onset autosomal dominant polycystic kidney disease, while biallelic *PKD1* variants are associated with

early and potentially neonatal-onset, severe polycystic kidney disease (Al-Hamed et al., 2019; Audrézet et al., 2016; Durkie et al., 2021). Heterozygous *DNAJB11* variants are associated with autosomal dominant polycystic kidney disease, while biallelic variants cause Ivemark II syndrome or renal-hepatic-pancreatic dysplasia syndrome (Jordan et al., 2021). We propose that *TOPORS* has similar properties, with heterozygous variants causing the milder, organ-specific ciliopathy retinitis pigmentosa, and biallelic variants causing OFDS-spectrum syndromic ciliopathy.

Our identified *TOPORS* patients both presented with the clinical stigmata of OFDS, including oral cavity malformations, dysmorphic features, and polydactyly; however, Patient 2 also presented with MTS, which is pathognomonic for JS. The overlap between OFDS and JS is well established, with several reports of individuals harboring features of both syndromes (Aljeaid et al., 2019; Bhardwaj et al., 2018; Johnston et al., 2017; Wentzensen et al., 2015). Several genes are associated with both conditions, including *C5ORF42*, *OFD1*, *TCTN3*, *TMEM107*, *TMEM216*, and *TMEM231*, and JS and OFDS can be allelic to each other (Bruel et al., 2017; Coene et al., 2009; Franco & Thauvin-Robinet, 2016). We propose that *TOPORS* also bridges OFDS and JS. It is unknown at this time whether this *TOPORS* phenotype is specific to the Pro10Gln variant identified in our probands, or whether it can be generalized to other gene variants. It is also unclear why Patient 3 and his affected sibling presented with neural tube defects while Patient 2 presented with MTS. Of note, both families trace their ancestry to the Dominican Republic, suggesting a possible founder allele.

In conclusion, we report on two novel genes associated with OFD VI, *TOPORS* and *CEP164*, further expanding the genetic differential of OFDS. Our cases highlight the phenotypic and genetic diversity of this family of diseases, and again implicate the ubiquitin-proteasome system in ciliary disease.

ACKNOWLEDGMENT

Medical Genetics Research Training Grant 5T32GM008638-22 (Alanna Strong) and Institutional Development Fund (Hakon Hakonarson).

CONFLICT OF INTEREST

None.

AUTHOR CONTRIBUTIONS

Alanna Strong conceptualized and designed the study, evaluated Patients 1 and 3 clinically, helped in variant interpretation and data analysis, and drafted the manuscript. Laurie Simone and Helio Fernando Pedro helped evaluate Patient 2 and helped analyze phenotypic and genetic data from all patients. Hayley Ron and Jennifer Kalish helped evaluate Patient 3 and guided the phenotypic workup. Elaine Zackai helped evaluate Patient 3, guide the phenotypic workup and interpret the genetic variants identified. Anthony Krentz helped analyze the exome for Patient 2. Deborah Watson and Courteney Vaccaro facilitated genetic data collection and analysis for Patient 3. Hakon Hakonarson helped conceptualize and design the study, contributed to data analysis, critically reviewed and edited the

manuscript, and provided funding for the work. All authors approved the final manuscript as submitted and agree to be accountable for all aspects of the work.

DATA AVAILABILITY STATEMENT

Data sharing is not applicable to this article as no new data were created or analyzed in this study.

ORCID

Alanna Strong  <https://orcid.org/0000-0001-9261-244X>

Jennifer M. Kalish  <https://orcid.org/0000-0003-1500-9713>

Hakon Hakonarson  <https://orcid.org/0000-0003-2814-7461>

REFERENCES

- Al-Hamed, M. H., Alshah, N., Rice, S. J., Edwards, N., Nooreddeen, E., Alotaibi, M., Kurdi, W., Alnemer, M., Altaieb, N., Ali, W., Al-Numair, N., Almejaish, N., Sayer, J. A., & Imtiaz, F. (2019). Biallelic PKD1 mutations underlie early-onset autosomal dominant polycystic kidney disease in Saudi Arabian families. *Pediatric Nephrology*, *34*(9), 1615–1623.
- Aljeaid, D., Lombardo, R. C., Witte, D. P., & Hopkin, R. J. (2019). A novel pathogenic variant in *OFD1* results in X-linked Joubert syndrome with orofaciocigital features and pituitary aplasia. *American Journal of Medical Genetics. Part A*, *179*(6), 1010–1014.
- Audrézet, M. P., Corbiere, C., Lebbah, S., Morinière, V., Broux, F., Louillet, F., Fischbach, M., Zalozyc, A., Cloarec, S., Merieau, E., Baudouin, V., Deschênes, G., Roussey, G., Maestri, S., Visconti, C., Boyer, O., Abel, C., Lahoche, A., Randrianaivo, H., ... Heidet, L. (2016). Comprehensive PKD1 and PKD2 mutation analysis in prenatal autosomal dominant polycystic kidney disease. *Journal of the American Society of Nephrology*, *27*(3), 722–729.
- Berbari, N. F., O'Connor, A. K., Haycraft, C. J., & Yoder, B. K. (2009). The primary cilium as a complex signaling center. *Current Biology*, *19*(13), R526–R535.
- Bhardwaj, P., Sharma, M., & Ahluwalia, K. (2018). Joubert syndrome with Orofacial digital features. *Journal of Neurosciences in Rural Practice*, *9*(1), 152–154.
- Bowne, S. J., Sullivan, L. S., Gire, A. I., Birch, D. G., Hughbanks-Wheaton, D., Heckenlively, J. R., & Daiger, S. P. (2008). Mutations in the *TOPORS* gene cause 1% of autosomal dominant retinitis pigmentosa. *Molecular Vision*, *14*, 922–927.
- Bruel, A. L., Franco, B., Duffourd, Y., Thevenon, J., Jegou, L., Lopez, E., Deleuze, J. F., Doummar, D., Giles, R. H., Johnson, C. A., Huynen, M. A., Chevrier, V., Burglen, L., Morleo, M., Desguerrès, I., Pierquin, G., Doray, B., Gilbert-Dussardier, B., Reversade, B., ... Thauvin-Robinet, C. (2017). Fifteen years of research on oral-facial-digital syndromes: From 1 to 16 causal genes. *Journal of Medical Genetics*, *54*(6), 371–380.
- Chakarova, C. F., Khanna, H., Shah, A. Z., Patil, S. B., Sedmak, T., Murgam-Zamalloa, C. A., Papaioannou, M. G., Nagel-Wolfrum, K., Lopez, I., Munro, P., Cheetham, M., Koenekoop, R. K., Rios, R. M., Matter, K., Wolfrum, U., Swaroop, A., & Bhattacharya, S. S. (2011). *TOPORS*, implicated in retinal degeneration, is a cilia-centrosomal protein. *Human Molecular Genetics*, *20*(5), 975–987.
- Chakarova, C. F., Papaioannou, M. G., Khanna, H., Lopez, I., Waseem, N., Shah, A., Theis, T., Friedman, J., Maubaret, C., Bujakowska, K., Veraitch, B., el-Aziz, M. M. A., Prescott, D. Q., Parapuram, S. K., Bickmore, W. A., Munro, P. M. G., Gal, A., Hamel, C. P., Marigo, V., ... Bhattacharya, S. S. (2007). Mutations in *TOPORS* cause autosomal dominant retinitis pigmentosa with perivascular retinal pigment epithelium atrophy. *American Journal of Human Genetics*, *81*(5), 1098–1103.

- Chaki, M., Airik, R., Ghosh, A. K., Giles, R. H., Chen, R., Slaats, G. G., Wang, H., Hurd, T. W., Zhou, W., Cluckey, A., Gee, H. Y., Ramaswami, G., Hong, C. J., Hamilton, B. A., Červenka, I., Ganji, R. S., Bryja, V., Arts, H. H., Van Rieuwijk, J., ... Hildebrandt, F. (2012). Exome capture reveals ZNF423 and CEP164 mutations, linking renal ciliopathies to DNA damage response signaling. *Cell*, 150(3), 533–548.
- Coene, K. L., Roepman, R., Doherty, D., Afroze, B., Kroes, H. Y., Letteboer, S. J., Ngu, L. H., Budny, B., van Wijk, E., Gorden, N. T., Azhimi, M., Thauvin-Robinet, C., Veltman, J. A., Boink, M., Kleefstra, T., Cremers, F. P., Van, B. H., & de Brouwer, A. P. (2009). OFD1 is mutated in X-linked Joubert syndrome and interacts with LCA5-encoded lebercilin. *American Journal of Human Genetics*, 85(4), 465–481.
- Daly, O. M., Gaboriau, D., Karakaya, K., King, S., Dantas, T. J., Lalor, P., Dockery, P., Krämer, A., & Morrison, C. G. (2016). CEP164-null cells generated by genome editing show a ciliation defect with intact DNA repair capacity. *Journal of Cell Science*, 129(9), 1769–1774.
- Durkie, M., Chong, J., Valluru, M. K., Harris, P. C., & Ong, A. C. M. (2021). Biallelic inheritance of hypomorphic PKD1 variants is highly prevalent in very early onset polycystic kidney disease. *Genetics in Medicine*, 23(4), 689–697.
- Franco, B., & Thauvin-Robinet, C. (2016). Update on oral-facial-digital syndromes (OFDS). *Cilia*, 5, 12.
- Fry, A. M., Leaper, M. J., & Bayliss, R. (2014). The primary cilium: Guardian of organ development and homeostasis. *Organogenesis*, 10(1), 62–68.
- Gerhardt, C., Lier, J. M., Burmühl, S., Struchtrup, A., Deutschmann, K., Vetter, M., Leu, T., Reeg, S., Grune, T., & Rütter, U. (2015). The transition zone protein Rpgrip1l regulates proteasomal activity at the primary cilium. *The Journal of Cell Biology*, 210(1), 115–133.
- Graser, S., Stierhof, Y. D., Lavoie, S. B., Gassner, O. S., Lamla, S., Le Clech, M., & Nigg, E. A. (2007). Cep164, a novel centriole appendage protein required for primary cilium formation. *The Journal of Cell Biology*, 179(2), 321–330.
- Gurrieri, F., Franco, B., Toriello, H., & Neri, G. (2007). Oral-facial-digital syndromes: Review and diagnostic guidelines. *American Journal of Medical Genetics. Part A*, 143A(24), 3314–3323.
- Haluska, P., Jr., Saleem, A., Rasheed, Z., Ahmed, F., Su, E. W., Liu, L. F., & Rubin, E. H. (1999). Interaction between human topoisomerase I and a novel RING finger/arginine-serine protein. *Nucleic Acids Research*, 27(12), 2538–2544.
- Izawa, I., Goto, H., Kasahara, K., & Inagaki, M. (2015). Current topics of functional links between primary cilia and cell cycle. *Cilia*, 4, 12.
- Johnston, J. J., Lee, C., Wentzensen, I. M., Parisi, M. A., Crenshaw, M. M., Sapp, J. C., Gross, J. M., Wallingford, J. B., & Biesecker, L. G. (2017). Compound heterozygous alterations in intraflagellar transport protein *CLUAP1* in a child with a novel Joubert and oral-facial-digital overlap syndrome. *Cold Spring Harbor Molecular Case Studies*, 3(4), a001321.
- Jordan, P., Arrondel, C., Bessières, B., Tessier, A., Attié-Bitach, T., Guterman, S., Morinière, V., Antignac, C., Saunier, S., Gubler, M. C., & Heidet, L. (2021). Bi-allelic pathogenic variations in *DNAJB11* cause Ivemark II syndrome, a renal-hepatic-pancreatic dysplasia. *Kidney International*, 99(2), 405–409.
- Kasahara, K., Kawakami, Y., Kiyono, T., Yonemura, S., Kawamura, Y., Era, S., Matsuzaki, F., Goshima, N., & Inagaki, M. (2014). Ubiquitin-proteasome system controls ciliogenesis at the initial step of axoneme extension. *Nature Communications*, 5, 5081.
- Lambacher, N. J., Bruel, A. L., van Dam, T. J., Szymańska, K., Slaats, G. G., Kuhns, S., McManus, G. J., Kennedy, J. E., Gaff, K., Wu, K. M., van der Lee, R., Burglen, L., Doummar, D., Riviére, F. B., Faivre, L., Attié-Bitach, T., Saunier, S., Curd, A., Curd, M., ... Blacque, O. E. (2016). *TMEM107* recruits ciliopathy proteins to subdomains of the ciliary transition zone and causes Joubert syndrome. *Nature Cell Biology*, 18(1), 122–131.
- Mohr, O. (1941). A hereditary lethal syndrome in man. *Avh Norske Videnskad Oslo*, 14, 1–18.
- Pan, Y. R., & Lee, E. Y. (2009). UV-dependent interaction between Cep164 and XPA mediates localization of Cep164 at sites of DNA damage and UV sensitivity. *Cell Cycle*, 8(4), 655–664.
- Parisi, M., & Glass, I. (2003). Joubert syndrome. In M. P. Adam, H. H. Ardinger, R. A. Pagon, et al. (Eds.), *GeneReviews*[®]. University of Washington, Seattle.
- Poretti, A., Vitiello, G., Hennekam, R. C., Arrigoni, F., Bertini, E., Borgatti, R., Brancati, F., D'Arrigo, S., Faravelli, F., Giordano, L., Huisman, T. A., Iannicelli, M., Kluger, G., Kyllerman, M., Landgren, M., Lees, M. M., Pinelli, L., Romaniello, R., Scheer, I. ... Boltshauser, E. (2012). Delineation and diagnostic criteria of oral-facial-digital syndrome type VI. *Orphanet Journal of Rare Diseases*, 7, 4.
- Pungaliya, P., Kulkarni, D., Park, H. J., Marshall, H., Zheng, H., Lackland, H., Saleem, A., & Rubin, E. H. (2007). TOPORS functions as a SUMO-1 E3 ligase for chromatin-modifying proteins. *Journal of Proteome Research*, 6(10), 3918–3923.
- Rajendra, R., Malegaonkar, D., Pungaliya, P., Marshall, H., Rasheed, Z., Brownell, J., Liu, L. F., Lutzker, S., Saleem, A., & Rubin, E. H. (2004). Topors functions as an E3 ubiquitin ligase with specific E2 enzymes and ubiquitinates p53. *The Journal of Biological Chemistry*, 279(35), 36440–36444.
- Shaheen, R., Ansari, S., Mardawi, E. A., Alshammari, M. J., & Alkuraya, F. S. (2013). Mutations in *TMEM231* cause Meckel-Gruber syndrome. *Journal of Medical Genetics*, 50(3), 160–162.
- Shamseldin, H. E., Shaheen, R., Ewida, N., Bubshait, D. K., Alkuraya, H., Almardawi, E., Howaidi, A., Sabr, Y., Abdalla, E. M., Alfaifi, A. Y., Alghamdi, J. M., Alsagheir, A., Alfares, A., Morsy, H., Hussein, M. H., al-Muhaizea, M. A., Shagrani, M., al Sabban, E., Salih, M. A., ... Alkuraya, F. S. (2020). The morbid genome of ciliopathies: An update. *Genetics in Medicine*, 22(6), 1051–1060.
- Siller, S. S., Sharma, H., Li, S., Yang, J., Zhang, Y., Holtzman, M. J., Winuthayanon, W., Colognato, H., Holdener, B. C., Li, F. Q., & Takemaru, K. I. (2017). Conditional knockout mice for the distal appendage protein CEP164 reveal its essential roles in airway multiciliated cell differentiation. *PLoS Genetics*, 13(12), e1007128.
- Sivasubramaniam, S., Sun, X., Pan, Y. R., Wang, S., & Lee, E. Y. (2008). Cep164 is a mediator protein required for the maintenance of genomic stability through modulation of MDC1, RPA, and CHK1. *Genes & Development*, 22(5), 587–600.
- Sobreira, N., Schiettecatte, F., Valle, D., & Hamosh, A. (2015). GeneMatcher: A matching tool for connecting investigators with an interest in the same gene. *Human Mutation*, 36(10), 928–930.
- Valente, E. M., Logan, C. V., Mougou-Zerelli, S., Lee, J. H., Silhavy, J. L., Brancati, F., Iannicelli, M., Travaglini, L., Romani, S., Illi, B., Adams, M., Szymanska, K., Mazzotta, A., Lee, J. E., Tolentino, J. C., Swistun, D., Salpietro, C. D., Fede, C., Gabriel, S., ... Gleeson, J. G. (2010). Mutations in *TMEM216* perturb ciliogenesis and cause Joubert, Meckel and related syndromes. *Nature Genetics*, 42(7), 619–625.
- Wentzensen, I. M., Johnston, J. J., Keppler-Noreuil, K., Acrich, K., David, K., Johnson, K. D., Graham, J. M., Jr., Sapp, J. C., & Biesecker, L. G. (2015). Exome sequencing identifies novel mutations in *C5orf42* in patients with Joubert syndrome with oral-facial-digital anomalies. *Human Genome Variation*, 2, 15045.
- Zhou, R., Wen, H., & Ao, S. Z. (1999). Identification of a novel gene encoding a p53-associated protein. *Gene*, 235(1–2), 93–101.

How to cite this article: Strong, A., Simone, L., Krentz, A., Vaccaro, C., Watson, D., Ron, H., Kalish, J. M., Pedro, H. F., Zackai, E. H., & Hakonarson, H. (2021). Expanding the genetic landscape of oral-facial-digital syndrome with two novel genes. *American Journal of Medical Genetics Part A*, 185A: 2409–2416. <https://doi.org/10.1002/ajmg.a.62337>